This is a “preproof” accepted article for *Mineralogical Magazine*.

This version may be subject to change during the production process.

10.1180/mgm.2024.96

Ferroinnelite, $Ba_4Ti_2Na(NaFe^{2+})Ti(Si_2O_7)_2[(SO_4)(PO_4)]O_2[O(OH)]$, a new mineral of the lamprophyllite group (seidozerite supergroup) from the Kovdor alkaline massif, Kola Peninsula, Russia: description and crystal structure and new data for innelite, $Ba_4Ti_2Na(NaMn^{2+})Ti(Si_2O_7)_2[(SO_4)(PO_4)]O_2[O(OH)]$

Elena Sokolova[1,*], Fernando Cámara[2], Frank C. Hawthorne[1], Giancarlo Della Ventura[3,4] and Simone Bernardini[3,4]

[1] Department of Earth Sciences, University of Manitoba, Winnipeg, Manitoba R3T 2N2, Canada;
[2] Dipartimento di Scienze della Terra “Ardito Desio”, Università degli Studi di Milano, Via Mangiagalli 34, 20133, Milano, Italy;
[3] Dipartimento di Scienze, Università di Roma Tre, Largo S. Leonardo Murialdo 1, I-00146 Roma, Italy;
[4] INFN-Laboratori Nazionali di Frascati (Roma), Italy

Running title: FERROINNELITE, A NEW MINERAL

* Corresponding author: elena.sokolova@umanitoba.ca

Abstract

Ferroinnelite, $Ba_4Ti_2Na(NaFe^{2+})Ti(Si_2O_7)_2[(SO_4)(PO_4)]O_2[O(OH)]$, is a new mineral from the Phlogopite deposit, Kovdor alkaline massif, Kola Peninsula, Russia. In an agpaitic pegmatite, ferroinnelite occurs as transparent elongated platy to tabular crystals up to 0.15 mm long. Associated minerals are cancrinite, orthoclase, aegirine-augite, magnesio-arfvedsonite, golyshevite and fluorapatite. The mineral is yellow to yellow brown with a vitreous luster and a white streak, $D_{calc.}$ is 4.088 g/cm^3. Ferroinnelite is triclinic, space group $P\bar{1}$, *a* 5.3994(8), *b* 7.09239(13), *c* 14.7345(4) Å, α 98.4086(19), β 94.3275(18), γ 90.0133(13)°, *V* 556.56(8) Å^3. The chemical composition of ferroinnelite is SO_3 5.47, Nb_2O_5 0.45, P_2O_5 4.59, ZrO_2 0.13, TiO_2 16.91, SiO_2 17.55, Al_2O_3 0.06, BaO 42.83, SrO 1.01, FeO 3.34, MnO 0.97, CaO 0.09, MgO 0.64, K_2O 0.01, Na_2O 4.47, H_2O 1.11, F 0.15, O = F –0.06, total 99.72 wt.%, with H_2O calculated from structure refinement. The empirical formula calculated on 26 (O + F) apfu is $(Na_{1.95}Fe^{2+}_{0.64}Mg_{0.21}Mn^{2+}_{0.19}Ca_{0.02})_{\Sigma 3.01}(Ba_{3.84}Sr_{0.13}Na_{0.03})_{\Sigma 4.00}(Ti_{2.91}Nb_{0.05}Al_{0.02}Zr_{0.01}Mg_{0.01})_{\Sigma 3.00}$ $Si_{4.02}S_{0.94}P_{0.89}H_{1.70}O_{25.89}F_{0.11}$, *Z* = 1. The crystal structure was refined to an R_1 index of 7.45% from 4485 unique reflections ($F_o > 4\sigma F$). The structure is a combination of a TS (titanium silicate) and an **I** (intermediate) blocks. The TS block consists of HOH sheets (H - heteropolyhedral, O - octahedral). The O sheet is composed of Ti-, Na- and (Na,Fe^{2+})-octahedra, the H sheet, of $^{[5]}$Ti-polyhedra and Si_2O_7 groups. The **I** block contains *T* sites, statistically occupied by S and P, and Ba atoms. Ideal compositions of the TS and **I** blocks are $\{Ti_2Na(NaFe^{2+})Ti(Si_2O_7)_2O_2[O(OH)]\}^{3-}$ and $\{Ba_4[(SO_4)(PO_4)]\}^{3+}$. Ferroinnelite is a new member of the lamprophyllite group of the seidozerite supergroup. It is isostructural with innelite-1*A*, $Ba_4Ti_2Na(NaMn^{2+})Ti(Si_2O_7)_2[(SO_4)(PO_4)]O_2[O(OH)]$. Ferroinnelite and innelite are related by the following cation substitution at the M^O3 site in the O sheet: $Fe^{2+}_{fer} \leftrightarrow Mn^{2+}_{inn}$. IR and Raman spectroscopies confirm presence of OH and H_2O groups in ferroinnelite and innelite.

Keywords*:* ferroinnelite, innelite-1*A*, crystal structure refinement, EMP analysis, IR and Raman spectroscopies, chemical formula, lamprophyllite group, seidozerite supergroup.

Introduction

This paper reports the description and crystal structure of ferroinnelite, ideally $Ba_4Ti_2Na(NaFe^{2+})Ti(Si_2O_7)_2[(SO_4)(PO_4)]O_2[O(OH)]$, a new mineral of the lamprophyllite group (seidozerite supergroup) from the Phlogopite deposit, Kovdor alkaline massif, Kola Peninsula, Russia. In 2008, we were looking for phosphoinnelite to do its crystal structure. We were working with a sample of phosphoinnelite from Kovdor from the mineral collection of the late Adriana and Renato Pagano, Milan, Italy (Collezione Mineralogica, sample 9530). We microprobed several crystals but could not find any crystal of phosphoinnelite, $Ba_4Na_3Ti_3Si_4O_{14}(PO_4,SO_4)_2(O,F)_3$, with P > S (Pekov *et al*., 2006). In sample 9530, we discovered a new mineral that we named ferroinnelite. We returned sample 9530 to Renato, except for several crystals that we had microprobed. Adriana and Renato Pagano passed away three years ago; since then, all our attempts to get hold of this sample failed. In this paper, we report experimental results obtained on three crystals of ferroinnelite: crystal 1 (0.120 x 0.100 x 0.025 mm) – crystal-structure refinement #1 and chemical analysis; crystal 2 (0.140 x 0.070 x 0.035 mm) – IR and Raman spectroscopies, crystal 3 (0.127 x 0.097 x 0.046 mm) – crystal-structure refinement #2. The new mineral and its name have been approved by the Commission on New Minerals, Nomenclature and Classification, International Mineralogical Association (IMA 2024-029). The holotype sample of ferroinnelite [a probe mount of the twinned crystal 1 (0.120 x 0.100 x 0.025 mm)] has been deposited in the collections of the Department of Natural History, Royal Ontario Museum (ROM), Toronto, Canada, catalogue number M61038.

Ferroinnelite is a Fe^{2+} structural analogue of innelite-1*A*, ideally $Ba_4Ti_2Na(NaMn^{2+})Ti(Si_2O_7)_2[(SO_4)(PO_4)]O_2[O(OH)]$ (Sokolova *et al*., 2011; Sokolova and Cámara, 2017).

General information on the seidozerite supergroup

There are currently fifty-two TS-block minerals (TS = Titanium Silicate) in the seidozerite supergroup (Memorandum 56-SM/16, Sokolova and Cámara, 2017), forty-five of which are listed in Sokolova and Cámara (2017); since then, surkhobite has been discredited (IMA 20-A), and eight new mineral species have been added: shkatulkalite, $Na_2Nb_2Na_3Ti(Si_2O_7)_2O_2(FO)(H_2O)_4(H_2O)_3$ (Men'shikov *et al*., 1996, Zolotarev *et al*., 2018, Sokolova *et al*., 2022a), selivanovaite, $Fe^{3+}\square Ti_2Na\square Ti_2(Si_2O_7)_2O_4(H_2O)_4$ (Pakhomovsky *et al*., 2018; Sokolova *et al*., 2022b), rinkite-(Y), $Ca_2(CaY)Na(NaCa)Ti(Si_2O_7)_2(OF)F_2$ (Pautov *et al*., 2019), fluorbarytolamprophyllite, $(BaK)Ti_2Na_3Ti(Si_2O_7)_2O_2F_2$ (Filina *et al*., 2019), bortolanite, $Ca_2(Ca_{1.5}Zr_{0.5})Na(NaCa)Ti(Si_2O_7)_2(OF)F_2$ (Day *et al*., 2022), nacareniobsite-(Y),

$Ca_2(CaY)Na_3Nb(Si_2O_7)_2(OF)F_2$ (Agakhanov *et al*., 2023), nacareniobsite-(Nd), $Ca_2(CaNd)Na_3Nb(Si_2O_7)_2(OF)F_2$ (IMA2023-012) and ferroinnelite (IMA2024-029).

The TS block is the main structural unit in all seidozerite-supergroup structures; it consists of a central O (Octahedral) sheet and two adjacent H (Heteropolyhedral) sheets; Si_2O_7 groups occur in the H sheets. The TS block is characterized by a planar minimal cell based on translation vectors, $\mathbf{t_1}$ and $\mathbf{t_2}$, the lengths of which are t_1 ~ 5.5 and t_2 ~ 7 Å, and $\mathbf{t_1} \wedge \mathbf{t_2}$ is close to 90°. Minerals of the seidozerite supergroup are divided into four groups based on the content of Ti and the topology and stereochemistry of the TS block: in the rinkite, bafertisite, lamprophyllite and murmanite groups, Ti (+ Nb + Zr + Fe^{3+} + Mg + Mn) = 1, 2, 3 and 4 apfu (atoms per formula unit) per $(Si_2O_7)_2$, respectively (Sokolova, 2006; Sokolova and Cámara, 2013, 2018). The seidozerite supergroup is based on a quantitative classification as minerals of each group have a fixed content of Ti (+ Nb + Zr + Fe^{3+} + Mg + Mn). Each group of minerals has a TS block with a different (1) content of Ti (+ Nb + Zr + Fe^{3+} + Mg + Mn), (2) topology defined by the type of linkage of H and O sheets, and (3) stereochemistry of Ti (+ Nb + Zr + Fe^{3+} + Mg + Mn) (Sokolova, 2006). There are three topologically distinct TS blocks based on three types of linkage of two H sheets and the central O sheet (Sokolova, 2006). *Linkage 1* occurs where two H sheets connect to the O sheet such that two Si_2O_7 groups on opposite sides of the O sheet link to *trans* edges of the same octahedron of the O sheet. *Linkage 2* occurs where two Si_2O_7 groups link to two octahedra of the O sheet adjacent along $\mathbf{t_2}$. *Linkage 3* occurs where two Si_2O_7 groups link to two octahedra adjacent approximately along $\mathbf{t_1}$. All TS-block structures consist either solely of TS blocks or of two types of block: the TS block and an **I** (Intermediate) block that comprises atoms between two TS blocks. Usually, the **I** block consists of alkali and alkaline-earth cations, H_2O groups and oxyanions $(PO_4)^{3-}$, $(SO_4)^{2-}$ and $(CO_3)^{2-}$. The general formula of the TS block is as follows: $A^P{}_2B^P{}_2M^H{}_2M^O{}_4(Si_2O_7)_2X_{4+n}$, where $M^H{}_2$ and $M^O{}_4$ are cations of the H and O sheets; M^H = Ti, Nb, Zr, Y, Mn, Ca + *REE*, Ca; M^O = Ti, Zr, Nb, Fe^{3+}, Fe^{2+}, Mg, Mn, Zn, Ca, Na; A^P and B^P are cations at the peripheral (*P*) sites = Na, Ca + *REE*, Ca, Zn, Ba, Sr, K; X are anions = O, OH, F, H_2O; $X_{4+n} = X^O{}_4 + X^P{}_n$, n = 0, 1, 1.5, 2, 4; $X^P = X^P{}_M$ and $X^P{}_A$ = apical anions of the M^H and A^P cations at the periphery of the TS block. There are four types of self-linkage between adjacent TS blocks (Sokolova, 2006): [1] TS blocks link directly through common edges of M^H and A^P polyhedra, and common vertices of M^H, A^P and Si polyhedra of the H sheets belonging to two TS blocks. [2] TS blocks link through common vertices of Ti(+ Nb) octahedra, and the **I** block has one layer of cations (m = 1). [3] TS blocks do not link directly, additional cations do not occur in the **I** space (m = 0), and TS blocks are connected through hydrogen bonds of H_2O groups at the X^P sites. [4] TS blocks do not link directly, and there are

additional layers of cations in the **I** block (m = 1–6).

Sokolova and Cámara (2013) introduced the concept of *basic* and *derivative structures* for TS-block minerals. A *basic structure* has the following four characteristics: (1) There is only one type of TS block. (2) The two H sheets of the TS block are identical. (3) There is only one type of **I** block or it is absent. (4) There is only one type of self-linkage of TS blocks. *Basic structures* obey the general structural principles of Sokolova (2006). A *derivative structure* has one or more of the three following characteristics: (1) There is more than one type of TS block. (2) There is more than one type of **I** block. (3) There is more than one type of self-linkage of TS blocks. A *derivative structure* is related to two or more *basic structures* of the same group: it can be derived by adding these structures via sharing of the central O sheet of the TS blocks of adjacent structural fragments which represent *basic structures*. There are five seidozerite-supergroup minerals with derivative structures, four of them occur in the lamprophyllite group.

In the lamprophyllite group, the TS block is characterised by Ti (+ Nb + Fe^{3+} + Mg) = 3 apfu; Ti occurs in the H sheets (2 apfu) and the O sheet (1 apfu). *Linkage 1* occurs: Si_2O_7 groups of the two H sheets link to trans edges of the Ti octahedron of the O sheet. In the crystal structures of the lamprophyllite-group minerals, TS blocks either alternate with **I** blocks, self-linkage [4] occurs or connect via hydrogen bonding between H_2O groups at the X^P sites, self-linkage [3] occurs.

Previous work on innelite

Kravchenko *et al.* (1961) described innelite, $(Na,Ca,Mg,Fe^{3+},Fe^{2+})_3(Ba,K,Mn)_4(Ti,Al)_3Si_4O_{24}(OH,F)_{1.5} \cdot 1.15S$, from the Inagli massif, Yakutia, Russia. They reported triclinic symmetry, a chemical analysis (they did not analyze innelite for phosphorous) and deposited the holotype sample at the Fersman Mineralogical Museum, Moscow, Russia (sample #81801, collections of S.M. Kravchenko and A.F. Efimov).

Chernov *et al.* (1971) solved the crystal structure of innelite on a single crystal from the holotype sample #81801, described the main features of the structure topology and wrote its ideal formula as $Na_2Ba_3(Ba,K,Mn)(Ca,Na)Ti(TiO_2)_2[Si_2O_7]_2(SO_4)_2$. Based on the structure work of Chernov *et al.* (1971), Sokolova (2006) considered innelite a TS-block mineral and wrote its ideal formula as $Na_2CaBa_4Ti_3[Si_2O_7]_2(SO_4)_2O_4$.

Pekov *et al.* (2006) reported a chemical composition for innelite from the Inagli and Kovdor massifs, emphasizing that innelite contains P (with S > P) and wrote an “ideal” formula of innelite as $Ba_4(Na,Ca)_3Ti_3Si_4O_{14}(SO_4)_2(O,OH,F)_4$; however, they did not list H_2O in the chemical analyses and did not include (PO_4) in the formula.

In 2008, we obtained a fragment of the holotype sample of innelite (#81801, Inagli, Yakutia, Russia, Fersman Mineralogical Museum) for a comprehensive study using single-crystal X-ray diffraction, EMPA and HRTEM. Transmission electron microscopy showed that the sample is an intergrowth of two innelite polytypes, and the crystal structures of innelite-1*T* (space group $P\bar{1}$) and innelite-2*M* (space group *P*2/*c*; $c_{2M} = 2c_{1T}$) were solved and refined (Sokolova *et al.*, 2011). The crystal structure of innelite is a combination of a TS block which consists of HOH sheets and an **I** block. The **I** block contains *T* sites, statistically occupied by S and P, and Ba atoms. Innelite-1*T* is innelite as described by Kravchenko *et al.* (1961) and Chernov *et al.* (1971). Sokolova *et al.* (2011) wrote the ideal structural formula of innelite as $Ba_4Ti_2\,Na(NaM^{2+})Ti(Si_2O_7)_2[(SO_4)(PO_4)]O_2[O(OH)]$, M^{2+} = Mn > Fe > Mg > Ca.

Sokolova and Cámara (2017) considered innelite a lamprophyllite-group (seidozerite-supergroup) TS-block mineral, redefined its formula based on the work of Sokolova *et al*. (2011) and renamed innelite-1*T* as innelite-1*A* (Memorandum 56-SM/16).

Later on, in the IMA list of minerals, the redefined formula of innelite was changed to $Ba_4Ti_2\,Na(NaCa)Ti(Si_2O_7)_2[(SO_4)(PO_4)]O_2[O(OH)]$. Recently, we pointed out that Mn^{2+} is the dominant divalent cation at the M^O3 site, not Ca. Thus, the formula of innelite was corrected to $Ba_4Ti_2Na(NaMn^{2+})Ti(Si_2O_7)_2\,[(SO_4)(PO_4)]O_2[O(OH)]$ (Bosi *et al*., 2024).

Occurrence and associated minerals

As we found ferroinnelite in a sample of “phosphoinnelite” (see above), information on occurrence, associated minerals and origin of ferroinnelite is taken from Pekov *et al*. (2006). Ferroinnelite occurs in an agpaitic pegmatite vein cross-cutting calcite carbonatite at the Phlogopite deposit, Kovdor alkaline massif, Kola Peninsula, Russia (67°35′21″ N and 30°28′4″ E). Associated minerals are cancrinite (partly altered to thompsonite-Ca), orthoclase, aegirine-augite, magnesio-arfvedsonite, golyshevite and fluorapatite. The mineral formed in a pegmatite as a result of hydrothermal activity.

Physical properties

Ferroinnelite occurs as transparent elongated platy to tabular crystals up to 0.15 mm long. Figure 1 shows a single crystal of ferroinnelite (0.140 x 0.070 x 0.035 mm) on a glass fibre. Ferroinnelite is yellow to yellow brown; very small grains are pale yellow. The mineral has a white streak and a vitreous lustre. Ferroinnelite does not fluoresce under cathode rays or ultraviolet light. The mineral is brittle, cleavage is {001} medium, the fracture is uneven; no

parting was observed. Mohs hardness is ~5 by analogy with innelite [4.75] (Kravchenko *et al*., 1961). The calculated density, $D_{calc.}$, is 4.088 g/cm^3.

Ferroinnelite is biaxial (+). The calculated mean refractive index of ferroinnelite is <*n*> = 1.823. Canadian safety regulations do not allow use of refractive-index liquids of 1.800 and above and so we cannot measure them. The optic angle, 2V = 87(2)°, was measured on a spindle stage using the method of extinction angles. Ferroinnelite is slightly pleochroic, very pale yellow to yellow brown.

FTIR and Raman spectroscopies

FTIR and Raman single-crystal spectra for ferroinnelite were collected on crystal 2. In particular, the IR spectrum was collected at INFN, Laboratori Nazionali di Frascati (Rome) using a Bruker Hyperion 3000 microscope attached to a Vertex V66 optical bench. Operating conditions were: 4 cm^{-1} nominal resolution on both peak and background, KBr beamsplitter, MCT N_2-cooled detector, averaging 128 scans. The beam size was ~50 x 50 μm^2. Raman measurements were done at the Raman Spectra Lab, Department of Science, Roma Tre University, at room temperature using an inVia Renishaw spectrometer equipped with a diode laser (532 nm, output power 100 mW), an edge filter, a 1800 lines per mm diffraction grating and a Peltier-cooled 1024 × 256 pixel CCD detector; the sample was mounted on the manual stage of a Leica DM2700 M confocal microscope. Spectral acquisitions (20 accumulations, 30 s each) were done with a 50× objective and a laser power of 3.5 mW.

A selected FTIR spectrum in the principal (OH)-stretching region of ferroinnelite is given in Fig. 2a, where it is compared with the spectrum collected for holotype innelite 81801 from Yakutia (Fig. 2b). Due to the very small size of the analyzed samples, both patterns are very noisy and poorly resolved, however both show undoubtedly the presence of OH groups in the structure. Both spectra consist of a peak at ~3630 cm^{-1} and a broad band due to several overlapping components, centered around 3550 cm^{-1} in ferroinnelite and 3590 cm^{-1} in innelite; these are superimposed on a very broad absorption centered at ~3310 cm^{-1} in ferroinnelite and ~3469 cm^{-1} in innelite that can be assigned to H_2O groups and eventually moisture adsorbed on the analyzed grains.

The Raman spectra (Fig. 2c and 2d) show a weak but well-defined (OH)-stretching pattern (see insets in Fig. 2c and 2d) where relatively sharp peaks are resolved at 3567–3591 cm^{-1} (for ferroiinelite and innelite, respectively) and 3643–3650 cm^{-1}; the higher wavenember peak of ferroinnelite is split with a second evident component at 3671 cm^{-1} (Fig. 2c). Two additional broad components at 3416–3439 cm^{-1} (for ferroiinelite and innelite, respectively), and

3153–3167 cm^{-1} can be related to H_2O. In the low-frequency range (<1200 cm^{-1}), the spectra are very similar and extremely complex and show five intense to relatively intense peaks at frequency > 800 cm^{-1} plus many lower-intensity peaks at frequencies < 800 cm^{-1}. Based on the literature data for similar TS-block minerals (*e.g.* Sokolova *et al*., 2015; Cámara *et al*., 2016), peaks at frequencies > 800 cm^{-1} can be assigned to Si–O stretching, whereas peaks at frequencies < 800 cm^{-1} can be assigned to Si–O bending and to M–O modes. Moreover, the spectra are complicated by the presence of SO_4 and PO_4 tetrahedra in the **I** block whose modes typically occur as intense scattering at frequencies > 900 cm^{-1}.

Chemical composition

The ferroinnelite crystal 1 previously used for single-crystal X-ray data collection was analyzed with a Cameca SX-100 electron-microprobe operating in wavelength-dispersion mode with an accelerating voltage of 15 kV, a specimen current of 20 nA, a beam size of 10 μm and count times on peak and background of 20 and 10 s, respectively. The following standards were used for K_α or L_α X-ray lines (analyzing crystals are given in brackets): F(LTAP): F-bearing riebeckite; Na(TAP): albite; Si(TAP), Ca(LPET): diopside; Nb(PET): $Ba_2NaNb_5O_{15}$; P(LPET): apatite; Ti(LLiF): titanite; Sr(LPET): $SrTiO_3$; Ta(LLiF): $MnNb_2Ta_2O_9$; Mn(LLiF): spessartine; Mg(TAP): forsterite; Fe(LLiF): fayalite; Zr(LPET): zircon; S(LPET), Ba(LiF, L_β): barite; Al(LTAP): andalusite; K(LPET): orthoclase. Data were reduced using the $\phi(\rho Z)$ procedure of Pouchou and Pichoir (1985). The chemical composition of ferroinnelite is given in Table 1 and is the mean of 11 determinations.

The empirical formula calculated on 26 (O + F) atoms per formula unit (apfu) is $(Na_{1.95}Fe^{2+}_{0.64}Mg_{0.21}Mn^{2+}_{0.19}Ca_{0.02})_{\Sigma 3.01}(Ba_{3.84}Sr_{0.13}Na_{0.03})_{\Sigma 4.00}(Ti_{2.91}Nb_{0.05}Al_{0.02}Zr_{0.01}Mg_{0.01})_{\Sigma 3.00}$ $Si_{4.02}S_{0.94}P_{0.89}H_{1.70}O_{25.89}F_{0.11}$, $Z = 1$. The structural formula based on assigned site-populations (see below) is $(Ba_{3.84}Sr_{0.13}Na_{0.03})_{\Sigma 4}(Ti_{1.98}Al_{0.02})_{\Sigma 2}Na(Na_{0.95}Fe^{2+}_{0.64}Mg_{0.21}Mn^{2+}_{0.1919}Ca_{0.01})_{\Sigma 2}$ $(Ti_{0.93}Nb_{0.05}Zr_{0.01}\,Mg_{0.01})_{\Sigma 1}(Si_2O_7)_2[(SO_4)_{0.94}(PO_4)_{0.89}(OH)_{0.51}(H_2O)_{0.17}]O_2[O_{1.04}(OH_{0.85}F_{0.11})_{\Sigma 0.96}]_{\Sigma 2}$. The simplified formula is $(Ba,Sr)_4Ti_2Na(Na,Fe^{2+},Mg,Mn^{2+})_2(Ti,Nb)(Si_2O_7)_2[(SO_4)(PO_4)]O_2$ $(O,OH)_2$. The ideal formula of ferroinnelite, $Ba_4Ti_2Na(NaFe^{2+})Ti(Si_2O_7)_2[(SO_4)(PO_4)]O_2[O(OH)]$, requires (wt.%): SO_3 5.77; P_2O_5 5.12; TiO_2 17.28; SiO_2 17.32; BaO 44.21; FeO 5.18; Na_2O 4.47; H_2O 0.65; Total 100.00.

X-ray powder diffraction

X-ray powder diffraction data were obtained by collapsing the entire dataset collected from the single crystal into one dimension. Data (in Å for Mo*K*α) are listed in Table 2. Unit-cell

parameters are therefore the same as for the single-crystal data (Table 3).

Crystal structure: experimental

Data collection and structure refinement

X-ray single-crystal data for ferroinnelite were collected from a twinned crystal (0.127 x 0.097 x 0.046 mm) with a Rigaku XtaLAB Synergy diffractometer, equipped with a PhotonJet-S (Mo) X-ray source operating at 50 kV and 1 mA, with monochromatized MoKα (0.71073 Å) radiation and equipped with a HyPix-6000HE Hybrid Photon Counting (HPC) detector working at 62 mm from the sample. The intensities of reflections with $–9 \le h \le 9$, $–12 \le k \le 12$, $–26 \le l \le 27$ were collected with a frame width of 0.5° and a frame time of 40 s up to $2\theta \le 81.44°$, and an empirical absorption correction (SCALE3 ABSPACK, Rigaku Oxford Diffraction, 2018) was applied. There were few observed reflections at high 2θ, and refinement of the structure was done for $2\theta \le 54°$, $–7 \le h \le 7$, $–9 \le k \le 9$, $–19 \le l \le 19$. The crystal structure was refined to $R_1 = 0.0745$ on the basis of 4485 unique reflections ($F_o > 4\sigma|F|$) using atom coordinates of innelite-1*A* (Sokolova *et al*., 2011) with Bruker SHELXTL version 2014/3 software (Sheldrick, 2015). The ratio of twin components is 0.466(2) : 0.534(2), and the twin matrix is (–1 0 0, 0 1 0, 0 0 –1). The occupancies of the Ti-dominant M^H and M^O1 sites were refined with the scattering factor of Ti; alkali-cation sites M^O2 with the scattering factor of Na and M^O3 with the scattering factor of Fe; Ba-dominant A^P and B^P sites with the scattering factor of Ba; *T* site with the scattering factor of S. The refined occupancy of the Ti-dominant M^O1 site is greater than 1 due to the presence of heavier cations such as Nb and Zr. That is why For the M^O2 site, site-occupancy refinement using the scattering factor of Na converged to 1.0 and was fixed at the last stages of the refinement. Neutral scattering factors were taken from the International Tables for X-ray Crystallography (Wilson, 1992). In the last stages of refinement, two subsidiary peaks were included in the refinement with the scattering factor of Ba. The presence of subsidiary peaks is a common feature in Ti silicates with the TS block; they are due to intimate intergrowths of these minerals and the presence of additional structure domains (see HRTEM results for innelite in Sokolova *et al*., 2011). Refined site-occupancies of subsidiary peaks were 2 and 3%. The details of X-ray data collection and structure refinement are given in Table 3, final atom parameters are given in Table 4, selected interatomic distances and angles in Table 5, refined site-scattering values and assigned site-populations in Table 6, and bond-valence values in Table 7. A CIF and a list of observed and calculated structure factors for ferroinnelite have been deposited with the Principal Editor of *Mineralogical Magazine* and are available as Supplementary Material (see below).

Site-population assignment

We divide the cation sites into 3 groups: M^{H} and *Si* sites of the H sheet, M^{O} sites of the O sheet, and *T*, A^{P} and B^{P} sites of the **I** block. Consider first the Ti (+ Nb)-dominant sites. In TS-block structures, Ti (+ Nb)-dominant sites are always fully occupied. Table 1 shows that the $2M^{H}$ and $1M^{O}$ sites are occupied by $Ti_{2.91}Nb_{0.05}Al_{0.02}Zr_{0.01}Mg_{0.01}$ apfu [66.85 epfu (electrons per formula unit)]. The aggregate refined scattering at these sites (66.6 epfu, Table 4–6) is in agreement with this composition. We assign $Ti_{1.98}Al_{0.02}$ to the M^{H} site and $Ti_{0.93}Nb_{0.05}Zr_{0.01}Mg_{0.01}$ to the $M^{O}1$ site (Table 6). Although the $2M^{H}$ and $1M^{O}$ sites are 99 and 93% occupied by Ti (see above), calculated bond-valence value at the Ti-dominant site in the O sheet is significantly low: 3.62 vu (valence units) when compared to aggregate charges of 3.99^{+} and 4.03^{+} for M^{H} and $M^{O}1$ sites, respectively (Table 7). Although Ti in the O sheet shows low incident bond-valence sums in several lamprophyllite-group minerals, this issue is not yet understood. Consider next the alkali-cation $M^{O}(2,3)$ sites in the O sheet (3 apfu). Table 1 gives $Na_{1.95}Fe^{2+}_{0.64}Mg_{0.21}Mn^{2+}_{0.19}Ca_{0.02}$, *i.e*. 3.01 apfu, with a total scattering of 45.76 epfu. The total refined scattering at the alkali sites is 44.0 epfu (Table 6). In accord with the occupancy refinement of the $M^{O}2$ site (see above), we assign Na to this site (Table 6). To the $M^{O}3$ site, we assign $Na_{0.95}(Fe^{2+}_{0.64}Mg_{0.21}Mn^{2+}_{0.19}Ca_{0.01})$, *i.e*. 2 apfu, (with a total scattering of 34.56 epfu) (Table 6).

Consider last the cation sites in the **I** block. We assign $S_{0.94}P_{0.89}\square_{0.17}$ pfu (Table 1) to the *T* site (Table 6). We assign Ba with minor Sr and Na to the peripheral A^{P} and B^{P} sites.

Structure description

Cation sites

Site nomenclature. The cation sites are divided into 3 groups: the M^{O} sites of the O sheet, the M^{H} and *Si* sites of the H sheet, and the peripheral A^{P} and B^{P} sites and the *T* sites in the **I** block. In accord with Sokolova (2006), we label X^{O}_{M} and X^{O}_{A} two anions of the O sheet which do not coordinate Si atoms; X^{O}_{M} = anion at the common vertices of 3 M^{O} and $^{[5]}M^{H}$ polyhedra; X^{O}_{A} = anion at the common vertices of 3 M^{O} octahedra.

O sheet. There are three cation sites in the O sheet: the $M^{O}1$, $M^{O}2$ and $M^{O}3$ sites are occupied by $Ti_{0.93}Nb_{0.05}Zr_{0.01}Mg_{0.01}$, Na and $[Na_{0.95}(Fe^{2+}_{0.64}Mg_{0.21}Mn^{2+}_{0.1964}Ca_{0.01})]$ apfu, respectively, and the ideal compositions of the $M^{O}1$, $M^{O}2$ and $M^{O}3$ sites are Ti, Na and $(NaFe^{2+})$ apfu (Table 6). The $M^{O}1$ and $M^{O}3$ cations are coordinated by four O atoms and two X^{O}_{A} anions (see *Anion considerations* below) with $<M^{O}1–\varphi> = 2.00$ Å and $<M^{O}3–\varphi> = 2.27$ Å (φ = O,OH,F) (Tables 4–6; Fig. 3a). The structure diagrams were drawn using Atoms 6.4 software (Dowty,

2016). The $M^{O}2$ cation is coordinated by six O atoms, with $<M^{O}2–O>$ = 2.43 Å (Table 5). The cations of the O sheet sum ideally to $Na(NaFe^{2+})Ti$ apfu.

H sheet. In the H sheet, there are two tetrahedrally coordinated *Si* sites, occupied by Si, with <Si–O> = 1.63 Å (Table 6, Fig. 3b). The [5]-coordinated M^{H} site is occupied mainly by Ti (Table 6) and is coordinated by O atoms, with $<M^{H}–O>$ = 1.92 Å; the very short $M^{H}–X^{O}_{M}$ distance of 1.70 Å (Table 5) is in accord with the structure topology of lamprophyllite-group minerals (Sokolova, 2006). For the two H sheets, the sum of the cations is ideally Ti_2Si_4 apfu.

***I** bloc*k. In the **I** block, there are two distinct peripheral A^P and B^P sites (Fig. 4). The [9]-coordinated A^P and [11]-coordinated B^P sites are occupied mainly by Ba (Table 6). The A^P and B^P sites are coordinated by O atoms of the H sheet and O atoms (or OH and H_2O groups) of the **I** block (see below), with $<A^P–\varphi>$ = 2.87 and $<B^P–\varphi>$ = 2.88 Å, respectively (Fig. 5a,b). The ideal composition of the two A^P and B^P sites is Ba_4 apfu. There is one *T* site occupied by $S_{0.94}P_{0.89}\square_{0.17}$ pfu, ideally (SP) apfu, and coordinated by four O atoms, with <T–O> = 1.50 Å (Tables 5,6; Figs. 4,5a). The three sites in the **I** block ideally give Ba_4(SP) apfu.

We write the cation part of the ideal formula as the sum of the cations of the **I** block + O sheet + two H sheets: Ba_4(SP) + $Na(NaFe^{2+})Ti$ + Ti_2Si_4 = $Ba_4Na(NaFe^{2+})Ti_3Si_4$(SP) with a total charge of 51^{+}.

Anion considerations

There are 13 anion sites in the crystal structure of ferroinnelite. In ferroinnelite, each anion site gives two anions pfu. Bond-valence values for anions are listed in Table 7. Seven anion sites, *O*(1–7), are occupied by O atoms which form the tetrahedral coordination of the Si atoms (Tables 4, 5). The $^{[4]}X^{O}_{M}$ anion receives bond-valence contributions from four cations: M^{H}(Ti), $M^{O}2$ (Na) and two $M^{O}3$ ($Na_{0.5}Fe^{2+}_{0.5}$), summing to 2.03 vu (Table 7) and it is an O atom (Figs. 3a,b). Hence O(1–7) + X^{O}_{M} anions sum to O_{16} apfu.

Short-range order at the X^{O}_{A} site. In ferroinnelite, the $^{[3]}X^{O}_{A}$ anion receives bond-valence contributions from three cations: $M^{O}1$ (Ti) and two $M^{O}3$ ($Na_{0.5}Fe^{2+}_{0.5}$) (Fig. 3a); note that the fourth cation, A^P, occurs at a distance of 3.53 Å and hence does not contribute. The X^{O}_{A} anion receives bond valence of 1.20 vu and, from a long-range perspective, would be considered a monovalent anion. However, let us take into consideration the short-range order (SRO) of cations at the adjacent $M^{O}3$ site, which is occupied by $Na_{0.475}M^{2+}_{0.525}$ [= $Na_{0.95}$ ($Fe^{2+}_{0.64}Mg_{0.21}$ $Mn^{2+}_{0.19}Ca_{0.01}$)$_{\Sigma 1.05}$ apfu]. Where the $M^{O}3$ site is occupied by M^{2+}, the adjacent X^{O}_{A} anion receives bond-valence from Ti at the $M^{O}1$ site and two M^{2+} at the $M^{O}3$ site (Fig. 3a), and the X^{O}_{A} site is locally occupied by $O^{2–}$. Where the $M^{O}3$ site is occupied by Na, the X^{O}_{A} anion receives

bond valence from Ti at the M^O1 site and two Na at the M^O3 site (Fig. 3a), and the X^O_A site is occupied by the monovalent anions, $(OH)^-$ and F^-. The M^O3 site composition is $Na_{0.475}M^{2+}_{0.525}$ [= $Na_{0.95}(Fe^{2+}_{0.64}Mg_{0.21}Mn^{2+}_{0.19}Ca_{0.01})_{\Sigma 1.05}$ apfu], and therefore the composition of the X^O_A site is $O_{0.52}(OH+F)_{0.48}$ [= $O_{1.04}(OH+F)_{0.96}$pfu]. Chemical analysis gives $F_{0.11}$ pfu (Table 1), and we write composition of the X^O_A site as $O_{1.04}(OH)_{0.85}F_{0.11}$ pfu, ideally [O(OH)] pfu. The corresponding bond valence incident at the X^O_A anion should be ~1.5 vu, and the lower value of 1.2 vu (Table 7) is probably due to the fact that dominance of Na at the M^O3 site is responsible for longer distances.

Short-range order of anions in the ***I*** *block.* In ferroinnelite, there are four anions, O(8–11), that coordinate the *T* site which is occupied by $S_{0.94}P_{0.89}\square_{0.17}$ (Table 6). These anions receive bond valences of 1.64–2.10 vu (Table 7), and hence are O atoms (Table 4). Ba atoms at the A^P and B^P sites and TO_4 tetrahedra link via O(8–11). Where the *T* site is 91.5% occupied by S and P [$(S,P)_{1.83}\square_{0.17}$], each of the O(8–11) anions is bonded to the T atom and three Ba atoms [O(8–10): A^P and $2B^P$] or one Ba atom [O11: B^P] (Table 5). The O(8–11) atoms give 0.915 x 4 = 3.66 O per TO_4 group or 1.83 x 4 O = 7.32 O per $S_{0.94}P_{0.89}$ pfu. Where the *T* site is 8.5% vacant, the anions at the *O*(8–11) sites receive bond-valence solely from Ba atoms, 0.84, 0.83, 0.62 and 0.33 vu, respectively (Table 7) compatible with OH groups at the *O*(8–10) sites and an H_2O group at the *O*11 site (Fig. 5b). Atom O11 has ADP max/min ratio of 17.4 prolate due to the occupancy of the *O*11 site by a [2]-coordinated O atom at 91.5% and a [1]-coordinated H_2O group at 8.5%; hence the O11 atom is extremely positionally disordered.

The total content of OH and H_2O groups is $(OH)_{0.51}(H_2O)_{0.17}$ pfu. Hence the anion content of the *O*(8–11) sites is $O_{7.32}$ (*T* site occupied) + $(OH)_{0.51}(H_2O)_{0.17}$ (*T* site vacant) = $O_{7.32}(OH)_{0.51}(H_2O)_{0.17}$ pfu.

We write the ideal anion part of the innelite structure as the sum of the anion sites: O_{16} (14 O atoms of Si_4 tetrahedra and 2 O atoms at the X^O_M site) + [O(OH)] (at the X^O_A site) + O_8 (**I** block) = $O_{25}(OH)$ pfu, with a total charge of 51^-. This is in accord with the ideal cation part of the structure, $Ba_4Na(NaFe^{2+})Ti_3Si_4(SP)$, with a total charge of 51^+.

Structure topology

The main features of the structure topology of the ferroinnelite are in accord with the crystal structure of innelite reported by Chernov *et al.* (1971) and refined by Sokolova *et al*. (2011). The structure is a combination of a TS block and an **I** block. The TS block consists of HOH sheets, and the O sheet is an octahedral close-packed sheet (Fig. 3a). In the H sheet, two Si tetrahedra link to form an Si_2O_7 group, and Si_2O_7 groups share vertices with the [5]-coordinated M^H

polyhedra (Fig. 3b). In ferroinnelite, the TS block exhibits *linkage* 1 and stereochemistry typical for the lamprophyllite group: two H sheets connect to the O sheet such that two Si_2O_7 groups link to *trans* edges of the Ti octahedron of the O sheet (Figs. 3b,4). The ideal composition of the TS block of the form $M^H{}_2M^O{}_4(Si_2O_7)_2(X^O{}_M)_2(X^O{}_A)_2$ is $\{Ti_2Na(NaFe^{2+})Ti(Si_2O_7)_2O_2[O(OH)]\}^{3-}$. In accord with Sokolova (2006), $M^H{}_2M^O{}_4(Si_2O_7)_2(X^O{}_M)_2(X^O{}_A)_2$ is the invariant core of the TS block in all TS-block structures. In ferroinnelite, the TS blocks alternate with intermediate **I** blocks. An **I** block is always intercalated between two TS blocks and cations of the **I** block form close-packed layers parallel to the TS block, where m denotes the number of those layers (Sokolova, 2006). In innelite, there is one type of **I** block where m = 3. In two m layers, Ba atoms at the A^P and B^P sites are arranged in a close-packed fashion where each atom is surrounded by six others at approximately equal distances of 5 Å. The third, central, layer is composed of T tetrahedra of ideal composition $[(SO_4)(PO_4)]$, where S : P = 1 : 1. In the **I** block of the ferroinnelite structure, Ba atoms connect via TO_4 tetrahedra where the *T* site is occupied by S and P or via OH and H_2O groups where the *T* site is vacant (Fig. 5). The ideal composition of the **I** block of the form $A^P{}_2B^P{}_2(TO_4)_2$ is $\{Ba_4[(SO_4)(PO_4)]\}^{3+}$.

Chemical formula

For ferroinnelite, we write the ideal structural formula of the form $A^P{}_2B^P{}_2M^H{}_2M^O{}_4(Si_2O_7)_2(TO_4)_2(X^O{}_M)_2(X^O{}_A)_2$ as the sum of the ideal compositions of the TS block and **I** blocks: $\{Ti_2Na(NaFe^{2+})Ti(Si_2O_7)_2O_2[O(OH)]\}^{3-} + \{Ba_4[(SO_4)(PO_4)]\}^{3+} = Ba_4Ti_2Na(NaFe^{2+})Ti(Si_2O_7)_2[(SO_4)(PO_4)]O_2[O(OH)]$, where $M^H{}_2$ = cations of the H sheet = Ti_2; $M^O{}_4$ = cations of the O sheet = $Na(NaFe^{2+})Ti$; $X^O{}_4$ = anions in the O sheet = $O_2[O(OH)]$; $A^P{}_2B^P{}_2$ = cations at the *P* (peripheral sites) which belong to the **I** block = Ba_4; central part of the **I** block = $(TO_4)_2 = [(SO_4)(PO_4)]$.

Above, we reported the empirical formula for ferroinnelite (Table 1) calculated on the basis of 26 (O + F) anions: $(Na_{1.95}Fe^{2+}{}_{0.64}Mg_{0.21}Mn^{2+}{}_{0.19}Ca_{0.02})_{\Sigma 3.01}(Ba_{3.84}Sr_{0.13}Na_{0.03})_{\Sigma 4.00}(Ti_{2.91}Nb_{0.05}Al_{0.02}Zr_{0.01}Mg_{0.01})_{\Sigma 3.00}Si_{4.02}S_{0.94}P_{0.89}H_{1.70}O_{25.89}F_{0.11}$, $Z = 1$ and the structural formula based on assigned site-populations $(Ba_{3.84}Sr_{0.13}Na_{0.03})_{\Sigma 4}(Ti_{1.98}Al_{0.02})_{\Sigma 2}Na(Na_{0.95}Fe^{2+}{}_{0.64}Mg_{0.21}Mn^{2+}{}_{0.1919}Ca_{0.01})_{\Sigma 2}(Ti_{0.93}Nb_{0.05}Zr_{0.01}Mg_{0.01})_{\Sigma 1}(Si_2O_7)_2[(SO_4)_{0.94}(PO_4)_{0.89}(OH)_{0.51}(H_2O)_{0.17}]O_2[O_{1.04}(OH_{0.85}F_{0.11})_{\Sigma 0.96}]_{\Sigma 2}$. The validity of the ideal formula is supported by the close agreement between the charges for specific groups of cations in the ideal and structural formulae: 8^+ for Ba_4 *versus* 7.97^+ for $(Ba_{3.84}Sr_{0.13}Na_{0.03})_{\Sigma 4}$; 8^+ for Ti_2 versus 7.98^+ for $(Ti_{1.98}Al_{0.02})$; 4^+ for $Na(NaFe^{2+})$ *versus* 4.05^+ for $Na(Na_{0.95}Fe^{2+}{}_{0.64}Mg_{0.21}Mn^{2+}{}_{0.1919}Ca_{0.01})$; 5^- for $[(SO_4)(PO_4)]$ *versus* 5.06^- for $[(SO_4)_{0.94}(PO_4)_{0.89}(OH)_{0.51}H_2O_{0.17}]$.

Summary

(1) The chemical composition of ferroinnelite has been determined. The ideal structural formula of ferroinnelite of the form $A^{P}_{2}B^{P}_{2}M^{H}_{2}M^{O}_{4}(Si_2O_7)_2(TO_4)_2(X^{O}_{M})_2\,(X^{O}_{A})_2$ is $Ba_4Ti_2Na(NaFe^{2+})Ti(Si_2O_7)_2[(SO_4)(PO_4)]O_2[O(OH)]$, where S : P = 1 : 1.

(2) Ferroinnelite, ideally $Ba_4Ti_2Na(NaFe^{2+})Ti(Si_2O_7)_2[(SO_4)(PO_4)]O_2[O(OH)]$, is a new representative of titanium disilicate minerals with the TS block and a new member of the lamprophyllite group (Ti + Nb = 3 apfu) of the seidozerite supergroup. Ferroinnelite belongs to the structure type B2(LG): B = basic, LG = lamprophyllite group.

(3) There are two substitutions in the O sheet of the TS block: $Na^{+} \leftrightarrow Fe^{2+}$ at the $M^{O}3$ site adjacent to the X^{O}_{A} site and $OH^{-} \leftrightarrow O^{2-}$ at the X^{O}_{A} site, and these couple as follows: $Na^{+} + OH^{-} \leftrightarrow Fe^{2+} + O^{2-}$.

(4) There are two substitutions in the **I** block: ${}^{T}(S,P) \leftrightarrow {}^{T}\square$ at the *T* site and $O^{2-} \leftrightarrow OH^{-}$ + minor H_2O at the anion sites which coordinate the *T* sites; they couple as follows: ${}^{T}(S,P) + O^{2-} \leftrightarrow {}^{T}\square + OH^{-}$ + minor H_2O.

(5) Ferroinnelite is isostructural with innelite-1*A*, ideally $Ba_4Ti_2Na(NaMn^{2+})Ti(Si_2O_7)_2[(SO_4)(PO_4)]O_2[O(OH)]$ (Sokolova *et al*., 2011; Sokolova and Cámara, 2017) (Table 8). Ferroinnelite and innelite are related by the following cation substitution at the $M^{O}3$ site in the O sheet in the TS block: $Fe^{2+}_{fer} \leftrightarrow Mn^{2+}_{inn}$.

(6) IR and Raman spectroscopies confirmed the presence of OH and H_2O groups in ferroinnelite and the holotype sample of innelite (sample 81801, Fersman Mineralogical Museum, Moscow, Russia.

Acknowledgements

We thank two anonymous reviewers and the Principal Editor Stuart Mills for the comments that helped to improve the manuscript. We are grateful to Dmitrii Belakovsky of the Fersman Mineralogical Museum, Moscow, Russia, for loan of the sample #81801 of innelite originally given to the Museum by S.M. Kravchenko and A.E. Efimov and used by Chernov *et al.* (1971) to solve the crystal structure of innelite. F.C. Hawthorne was supported by a Discovery grant from the Natural Sciences and Engineering Research Council of Canada. F.C. Cámara was supported by the Italian Ministry of University (MIUR) through the project “Dipartimenti di Eccellenza 2023–2027”.

Supplementary material. To view supplementary material for this article, please visit https://doi.org/...

Competing interests. The authors declare none.

References

Agakhanov A.A., Day M.C., Sokolova E., Karpenko V.Yu., Hawthorne F.C., Pautov L.A., Pekov I.V., Kasatkin A.V. and Agakhanova V.A. (2023) Two rinkite-group (seidozerite-supergroup) minerals: nacareniobsite-(Y), a new mineral from the Darai-Pioz alkaline massif, Tajikistan and crystal-structure refinement of nacareniobsite-(Ce). *The Canadian Journal of Mineralogy and Petrology*, **61**, 1123–1136.

Bosi F., Hatert F., Pasero M. and Mills S. (2024) IMA Commission on New Minerals, Nomenclature and Classification (CNMNC) Newsletter 76. *Mineralogical Magazine*, **88**, 105–109.

Brown I.D. (1981) The bond-valence method: an empirical approach to chemical structure and bonding. Pp. 1–30 in: *Structure and Bonding in Crystals II* (M. O'Keeffe and A. Navrotsky, editors). Academic Press, New York.

Cámara F., Sokolova E., Abdu Y.A. and Pautov L.A. (2016) From structure topology to chemical composition. XIX. Titanium silicates: revision of the crystal structure and chemical formula of bafertisite, $Ba_2Fe^{2+}_4Ti_2(Si_2O_7)_2O_2(OH)_2F_2$, a Group-II TS-block mineral. *The Canadian Mineralogist*, **54**, 49–63.

Chernov A.N., Ilyukhin V.V., Maksimov B.A. and Belov N.V. (1971) Crystal structure of innelite, $Na_2Ba_3(Ba,K,Mn)(Ca,Ba)Ti(TiO_2)_2[Si_2O_7]_2(SO_4)_2$. *Soviet Physics Crystallography*, **16**, 65–69.

Day M.C., Sokolova E., Hawthorne F.C., Horváth L. and Pfenninger-Horváth E. (2022) Bortolanite, $Ca_2(Ca_{1.5}Zr_{0.5})Na(NaCa)Ti(Si_2O_7)_2(FO)F_2$, a new rinkite-group (seidozerite-supergroup) TS-block mineral from the Bortolan quarry, Poços De Caldas massif, Minas Gerais, Brazil. *The Canadian Mineralogist*, **60**, 699–712.

Dowty E. (2016) Atoms (Version 6.5.0). Shape Software, Kingsport, Tennessee, USA.

Filina M.I., Aksenov S.M., Sorokhtina N.V., Chukanov N.V., Kononkova N.N., Belakovskiy D.I., Britvin S.N., Kogarko L.N., Chervonnyi A.D. and Rastsvetaeva R.K. (2019) The new mineral fluorbarytolamprophyllite, $(Ba,Sr,K)_2[(Na,Fe^{2+})_3TiF_2][Ti_2(Si_2O_7)_2O_2]$ and chemical evolution of lamprophyllite-group minerals in agpaitic syenites of the Kola Peninsula. *Mineralogy and Petrology*, **113**, 533–553.

Kravchenko S.M., Vlasova E.V., Kazakova M.E., Ilyukhin V.V. and Abrashev K.K. (1961) Innelite, a new barium silicate. *Doklady Akademii Nauk SSSR*, **141**, 1198–1199 (in Russian).

Men'shikov Yu.P., Khomyakov A.P., Polezhaeva L.I. and Rastsvetaeva R.K. (1996) Shkatulkalite, $Na_{10}MnTi_3Nb_3(Si_2O_7)_6(OH)_2F \cdot 12H_2O$ - a new mineral. *Zapiski*

Vserossiiskogo Mineralogicheskogo Obshchestva, **125**(5), 120–126 (in Russian).

Pakhomovsky Y.A., Panikorovskii T.L., Yakovenchuk V.N., Ivanyuk G.Yu., Mikhailova Ju.A., Krivovichev S.V., Bocharov V.N. and Kalashnikov A.O. (2018) Selivanovaite, $NaTi_3(Ti,Na,Fe,Mn)_4[(Si_2O_7)_2O_4(OH,H_2O)_4]\cdot nH_2O$, a new rock-forming mineral from the eudialyte-rich malignite of the Lovozero alkaline massif (Kola Peninsula, Russia). *European Journal of Mineralogy*, **30**, 525–535.

Pautov L.A., Agakhanov A.A., Karpenko V.Yu., Uvarova Yu.A., Sokolova E. and Hawthorne F.C. (2019) Rinkite-(Y), $Na_2Ca_4YTi(Si_2O_7)_2OF_3$, a seidozerite-supergroup TS-block mineral from the Darai-Pioz alkaline massif, the Tien-Shan mountains, Tajikistan: Description and crystal structure. *Mineralogical Magazine*, **83**, 373–380.

Pekov I.V., Chukanov N.V., Kulikova I.M. and Belakovsky D.I. (2006) Phosphoinnelite, $Ba_4Na_3Ti_3Si_4O_{14}(PO_4,SO_4)_2(O,F)_3$, a new mineral from agpaitic pegmatites of Kovdor massif, Kola Peninsula. *Zapiski Vsesoyuznogo Mineralogicheskogo Obshchestva,* **135**(3), 52–60 (in Russian).

Pouchou J.L. and Pichoir F. (1985) 'PAP' φ(ρZ) procedure for improved quantitative microanalysis. Pp. 104–106 in: *Microbeam Analysis* (J.T. Armstrong, editor). San Francisco Press, California.

Raade G. and Berg H.-J. (2000) Powder X-ray diffraction data for innelite. *Powder Diffraction*, **15**, 62–64.

Rigaku Oxford Diffraction (2018) CrysAlisPro. Version 1.171.40.36a. Rigaku Oxford Diffraction, The Woodlands, Texas, USA.

Sheldrick G.M. (2015) Crystal Structure refinement with *SHELX*. *Acta Crystallographica*, **C71**, 3–8.

Sokolova E. (2006) From structure topology to chemical composition. I. Structural hierarchy and stereochemistry in titanium disilicate minerals. *The Canadian Mineralogist*, **44,** 1273–1330**.**

Sokolova E. and Cámara F. (2013) From structure topology to chemical composition. XVI. New developments in the crystal chemistry and prediction of new structure topologies for titanium disilicate minerals with the TS block. *The Canadian Mineralogist*, **51**, 861–891.

Sokolova E. and Cámara F. (2017) The seidozerite supergroup of TS-block minerals: nomenclature and classification, with change of the following names: rinkite to rinkite-(Ce), mosandrite to mosandrite-(Ce), hainite to hainite-(Y) and innelite-1*T* to innelite-1*A*. *Mineralogical Magazine*, **81**, 1457–1484.

Sokolova E. and Cámara F. (2018) From structure topology to chemical composition. XXV: new

insights into the close packing of cations in the structures of the seidozerite-supergroup TS-block minerals. *Zeitschrift für Kristallographie*, **233**(3–4), 205–221.

Sokolova E., Cámara F. and Hawthorne F.C. (2011) From structure topology to chemical composition. XI. Titanium silicates: crystal structures of innelite-1*T* and innelite-2*M* from Inagli massif, Yakutia, Russia, and the crystal chemistry of innelite. *Mineralogical Magazine,* **75**, 2495–2518.

Sokolova E., Abdu Y.A., Hawthorne F.C., Genovese A., Cámara F. and Khomyakov A.P. (2015) From structure topology to chemical composition. XVIII. Titanium silicates: revision of the crystal structure and chemical formula of betalomonosovite, a Group-IV TS-block mineral from the Lovozero alkaline massif, Kola Peninsula, Russia. *The Canadian Mineralogist,* **53**, 401–428.

Sokolova E., Day M.C., Hawthorne F.C. and Cámara F. (2022a) From structure topology to chemical composition. XXX. Refinement of the crystal structure and chemical formula of shkatulkalite, $Na_2Nb_2Na_3Ti(Si_2O_7)_2O_2(FO)(H_2O)_4(H_2O)_3$, a lamprophyllite-group (seidozerite-supergroup) TS-block mineral from the Lovozero massif, Kola Peninsula, Russia. *The Canadian Mineralogist*, **60**, 493–512.

Sokolova E., Day M.C., Hawthorne F.C. and Cámara F. (2022b) From structure topology to chemical composition. XXXI. Refinement of the crystal structure and chemical formula of selivanovaite, $NaFe^{3+}Ti_4(Si_2O_7)_2O_4(H_2O)_4$, a murmanite-group (seidozerite-supergroup) TS-block mineral from the Lovozero massif, Kola Peninsula, Russia. *The Canadian Mineralogist*, **60**, 513–531.

Wilson A.J.C. (editor) (1992) International Tables for Crystallography. Volume C: Mathematical, physical and chemical. Kluwer Academic Publishers, Dordrecht, The Netherlands.

Zolotarev Jr. A.A., Selivanova E.A., Krivovichev S.V., Savchenko Y.E., Panikorovskii T.L., Lyalina L.M., Pautov L.A. and Yakovenchuk V.N. (2018) Shkatulkalite, a rare mineral from the Lovozero Massif, Kola Peninsula: a re-investigation. *Minerals*, **8**, 303–314.

Figure captions

Fig. 1. Pale brownish-yellow crystal of ferroinnelite (0.140 x 0.070 x 0.035 mm) on a glass fibre. This crystal was used for IR-spectroscopy at INFN-Laboratori Nazionali di Frascati (Roma), Italy.

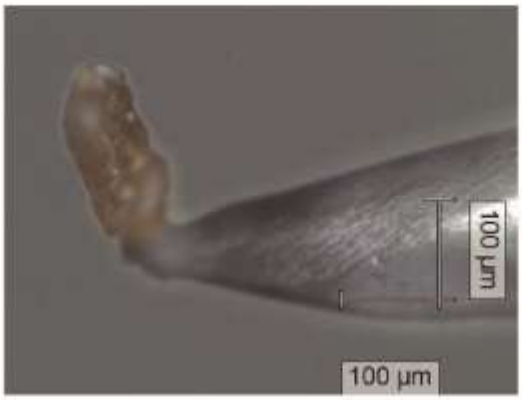

Fig. 1

Fig. 2. Infrared spectra of (a) ferroinnelite (crystal 9530_2) and (b) holotype innelite (crystal 81801_1) in the principal OH-stretching region; Raman spectra of (c) ferroinnelite and (d) holotype innelite from ~100 to 4000 cm^{-1}; the OH stretching range is shown in the inset where the pattern decomposition is given as a guide to the eye.

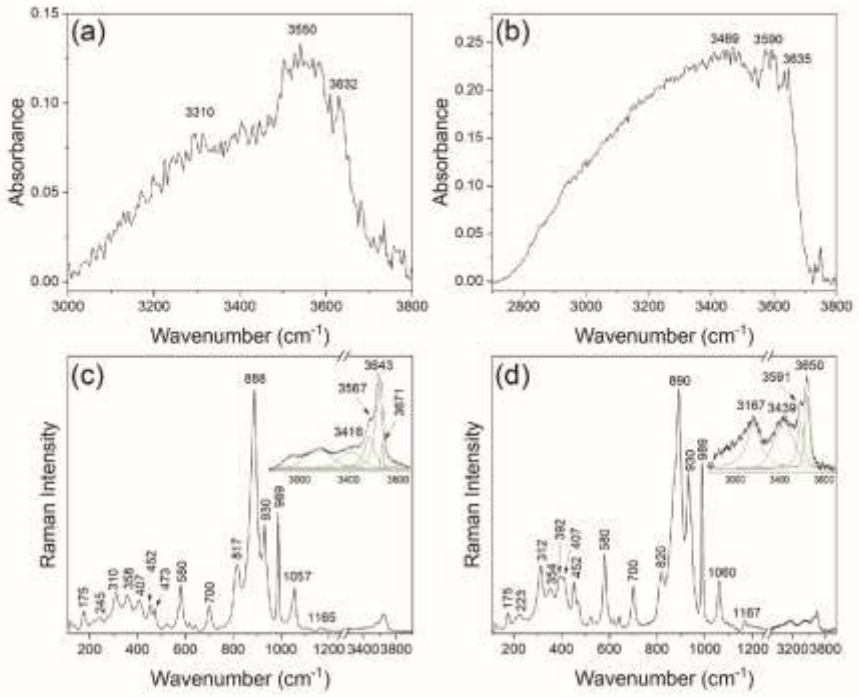

Fig. 2

Fig. 3. The TS block in the crystal structure of ferroinnelite viewed down [001]: (a) O sheet and (b) linkage of H and O sheets; SiO_4 tetrahedra are orange, Ti^{4+}-dominant polyhedra are yellow, Na octahedra and (Na,Fe^{2+}) octahedra are navy blue and bluish-green, respectively; X^{O}_{M} [O] and X^{O}_{A} [O,(OH)] anions are shown as small white circles with green rims and pink spheres. Labels 1 and 2 (on orange) correspond to Si(1,2) tetrahedra, respectively. Labels 1–3 correspond to M^{O}(1–3) octahedra in the O sheet, respectively. Inset on the right shows a possible hydrogen bond X^{O}_{A}–O3 where the $M^{O}3$ site is occupied by Na and the X^{O}_{A} site is occupied by an OH group shown as a small red sphere.

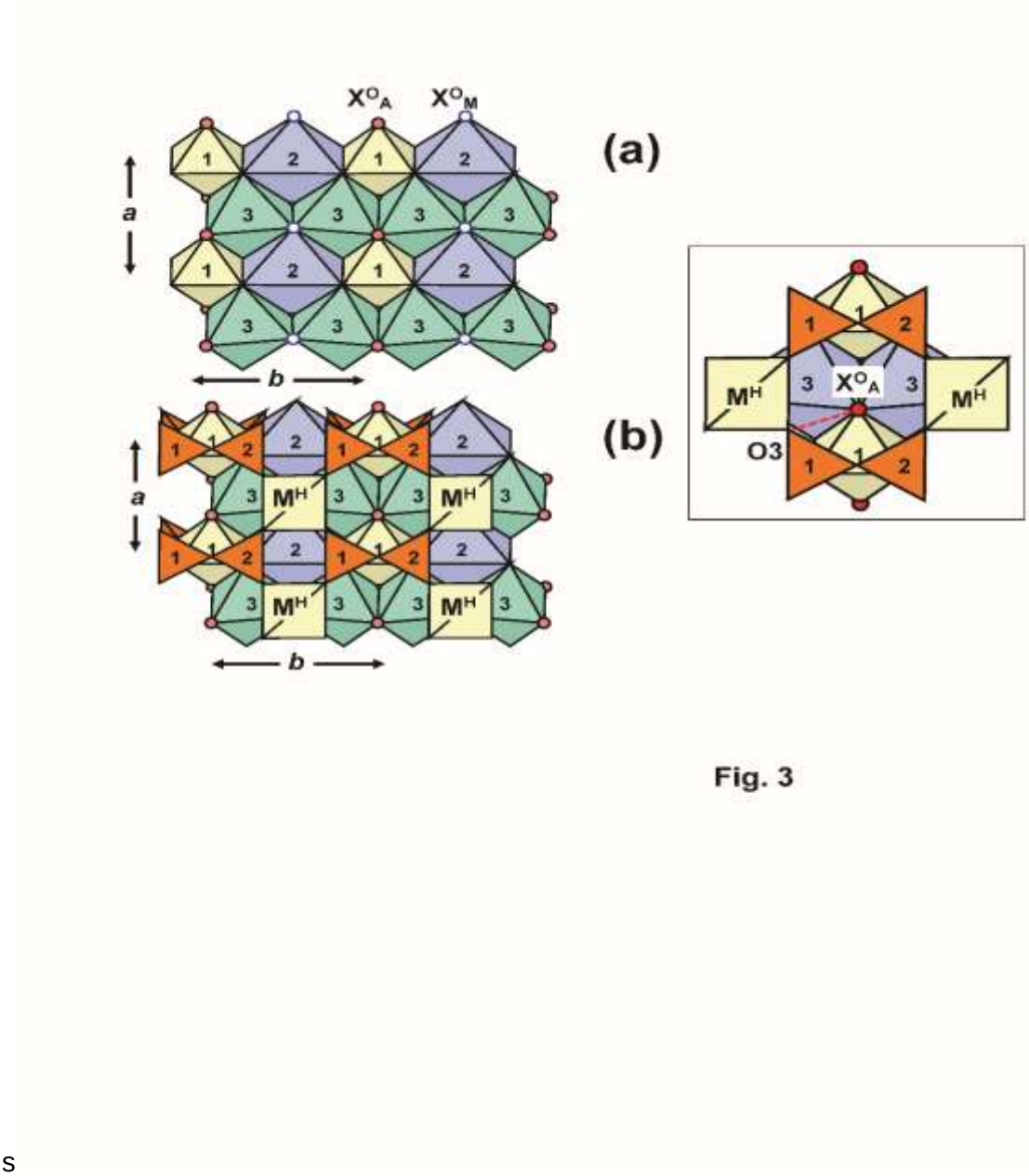

Fig. 3

S

Fig. 4. The crystal structure of ferroinnelite projected onto (100). Legend as in Fig. 3; Ba atoms at the A^P and B^P sites are shown as raspberry-coloured spheres, TO_4 (T = S,P) tetrahedra are yellow. The three vertical lines show the positions of the cation layers (m = 3) in the **I** block.

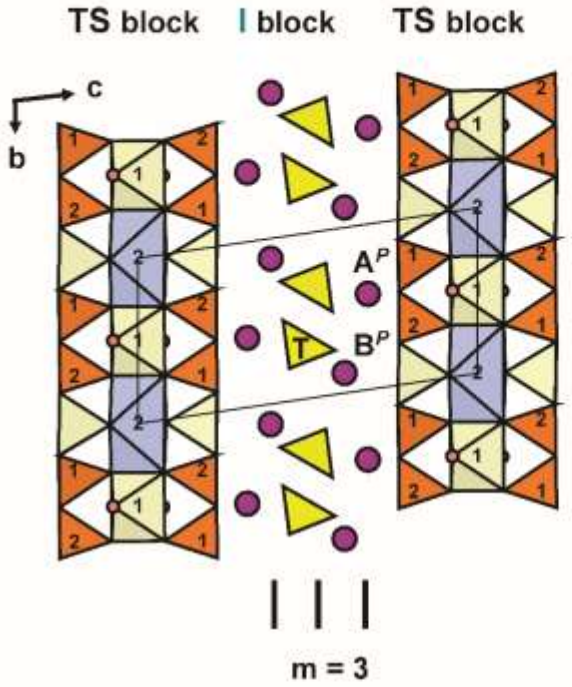

Fig. 4

Fig. 5. Details of short-range order of anions in the **I** block for ferroinnelite: (a) linkage of Ba atoms (at the $^{[9]}A^{P}$ and $^{[11]}B^{P}$ sites) and TO_4 tetrahedra where T tetrahedra are fully occupied by S and P; (b) linkage of Ba atoms at the A^{P} and B^{P} sites via OH [O(8,9,10)] and H_2O groups [O11] where *T* sites are vacant. Legend as in Fig. 4; Ba atoms at the A^{P} and B^{P} sites are shown as raspberry-colored spheres and labeled A and B, respectively. Anions in the **I** block are (a) not shown where they are O atoms which coordinate *T* sites occupied by S and P and (b) shown as small red OH and large red H_2O spheres where *T* sites are vacant. Thin black lines in (a) and (b) show Ba–O bonds; dashed lines in (b) show possible hydrogen bonds.

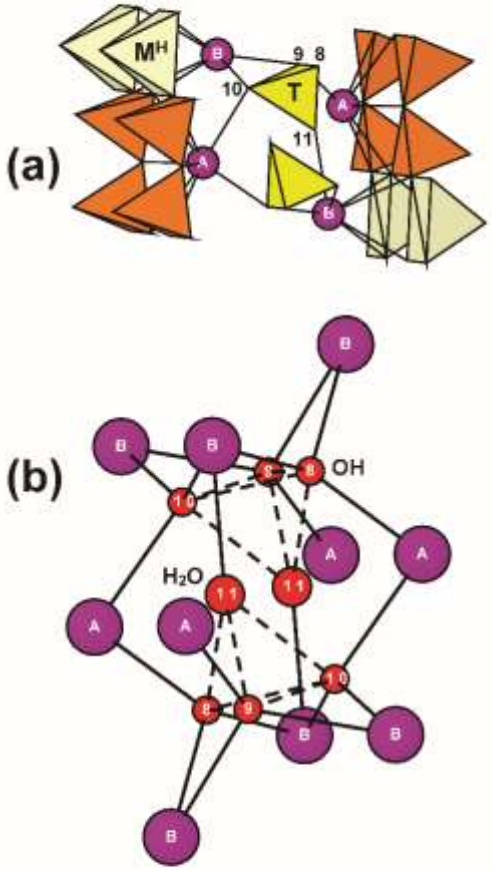

Fig. 5

Table 1. Chemical composition (wt.%) and unit formula (apfu) for ferroinnelite[1] and innelite[2].

Oxide	ferroinnelite	innelite	Formula unit	ferroinnelite	innelite
SO_3	5.47	6.03	S	0.94	1.02
Nb_2O_5	0.45	0.18	P	0.89	0.81
P_2O_5	4.59	4.24	Si	4.02	4.01
ZrO_2	0.13	n.d.			
TiO_2	16.91	17.50	Ti	2.91	2.97
SiO_2	17.55	17.76	Nb	0.05	0.02
Al_2O_3	0.06	0.06	Al	0.02	0.02
BaO	42.83	44.59	Zr	0.01	0
SrO	1.01	0.48	Mg	0.01	0
FeO	3.34	0.89	$\Sigma 2M^{H} + M^{O}$	3.00	3.01
MnO	0.97	1.98			
CaO	0.09	0.40	Na	1.95	2.16
MgO	0.64	0.43	Fe^{2+}	0.64	0.17
K_2O	0.01	0.00	Mg	0.21	0.15
Na_2O	4.47	4.95	Mn^{2+}	0.19	0.38
H_2O*	1.11	1.22	Ca	0.02	0.10
F	0.15	0.30	$\Sigma 3M^{O}$	3.01	2.96
O=F	–0.06	–0.13			
Total	99.72	100.88	Ba	3.84	3.94
			Sr	0.13	0.06
			Na	0.03	0.06
			$\Sigma 2A^{P} + 2B^{P}$	4.00	4.00
			Σ cations	15.86	15.81
			OH	0.85	0.99
			F	0.11	0.21
			$\Sigma 2X^{O}{}_{A}$**	0.96	1.20
			H***	0.85	0.85
			Total H^{+}	1.70	1.84

[1] this work: EMPA; [2] Sokolova *et al*. (2011): EMPA;
* calculated from structure-refinement results: [1][$(OH)_{1.36}$ and $(H_2O)_{0.17}$] and [2][$(OH)_{1.50}$ and $(H_2O)_{0.17}$] pfu;
** monovalent anions of the O sheet;
*** content of H^{+} in the **I** block from: [1][$(OH)_{0.51}(H_2O)_{0.17}$] and [2][$(OH)_{0.51}(H_2O)_{0.17}$] pfu

Table 2. Simulated X-ray powder diffraction data* for ferroinnelite.

$I_{est.}$	d_{calc} (Å)	*h*	*k*	*l*			
38	14.555	0	0	1			
6	11.449						
4	8.079						
6	7.116	0	0	2			
5	4.859	0	0	3			
13	4.156	1	$\bar{1}$	1			
22	3.934	$\bar{1}$	$\bar{1}$	2			
10	3.546	0	$\bar{2}$	1			
56	3.353	0	$\bar{2}$	2			
5	3.173	1	$\bar{1}$	$\bar{3}$			
8	3.045	0	$\bar{1}$	$\bar{4}$			
9	2.982	1	1	$\bar{4}$			
19	2.776	1	2	1			
100	2.694	2	0	0			
17	2.250	0	$\bar{3}$	1			
46	2.124	2	2	$\bar{2}$,	2	2	0
17	2.055	2	2	1,	2	$\bar{1}$	4
11	1.991	1	$\bar{2}$	$\bar{5}$,	1	3	$\bar{4}$
6	1.839	0	3	4,	0	$\bar{3}$	6
11	1.775	0	$\bar{4}$	1,	1	$\bar{2}$	7
5	1.642	3	1	2			
6	1.594	3	$\bar{2}$	1,	3	2	0
7	1.568	3	1	$\bar{5}$,	2	1	$\bar{8}$
10	1.480	2	$\bar{4}$	0,	2	$\bar{3}$	$\bar{5}$
2	1.430	3	3	$\bar{1}$			
7	1.365	2	$\bar{4}$	5,	1	$\bar{5}$	2
4	1.308	1	$\bar{4}$	8,	1	$\bar{4}$	$\bar{6}$

* the entire dataset of images was collapsed in 1D.

Table 3. Miscellaneous refinement data for ferroinnelite.

a (Å)	5.3994(8)
b	7.09239(13)
c	14.7345(4)
α (°)	98.4086(19)
β	94.3275(18)
γ	90.0133(13)
V (Å^3)	556.56(8)
Space group	$P\bar{1}$
Z	1
Reflections for cell refinement ($I > 10\sigma I$)	12004
Absorption coefficient (mm^{-1})	9.07
F(000)	627.9
$D_{calc.}$ (g/cm^3)	4.094
Crystal size (mm)	0.127 x 0.097 x 0.046
Radiation/monochromator	MoKα/graphite
2θ-range for structure refinement (°)	5.61 – 54.96
h *k* *l*	$-7 \le h \le 7$ $-9 \le k \le 9$ $-19 \le l \le 19$
R(σ) (%)	2.34
Ratio of twin components*	0.466(2) : 0.534(2)
Reflections collected	11786
Independent reflections $F_o > 4\sigma F$	4736 4485
Refinement method	Full-matrix least squares on F^2, fixed weights proportional to $1/\sigma F_o^2$
Final *R*(obs) (%)	
$F_o > 4\sigma F$	7.45
R_1	7.68
wR_2	20.95
Highest peak, deepest hole (e Å^{-3})	3.05, –2.03
Goodness of fit on F^2	1.140

* twin matrix is (–1 0 0 0 1 0 0 0 –1)

Table 4. Atom coordinates and anisotropic displacement parameters (Å^2) for ferroinnelite.

Atom	*x*	*y*	*z*	U^{11}	U^{22}	U^{33}	U^{23}	U^{13}	U^{12}	U_{eq}
Si1	0.8138(6)	0.2287(5)	0.8099(2)	0.0049(14)	0.0088(15)	0.0122(16)	0.0028(13)	0.0003(12)	–0.0008(13)	0.0085(7)
Si2	0.8156(7)	0.6607(5)	0.8121(3)	0.0081(15)	0.0069(15)	0.0134(16)	0.0040(13)	0.0010(13)	–0.0013(13)	0.0092(7)
M^H	0.6859(4)	0.0575(3)	0.19980(16)	0.0038(9)	0.0086(10)	0.0153(11)	0.0035(9)	0.0003(8)	–0.0011(8)	0.0091(5)
M^O10		½	0	0.030(2)	0.0141(18)	0.026(2)	0.0034(16)	–0.0137(15)	–0.0028(16)	0.0241(11)
M^O20		0	0	0.013(4)	0.030(5)	0.022(4)	0.005(4)	0.002(3)	0.002(4)	0.0215(18)
M^O3	0.4989(7)	0.7384(5)	0.9999(3)	0.0150(15)	0.0209(17)	0.0253(18)	0.0021(14)	0.0039(12)	0.0007(13)	0.0204(9)
T	0.7542(7)	0.2972(6)	0.5223(3)	0.0087(16)	0.0132(17)	0.0191(18)	0.0029(14)	0.0017(14)	–0.0004(13)	0.0136(8)
A^P	0.28690(17)	0.42085(14)	0.67782(8)	0.0136(4)	0.0152(5)	0.0458(6)	–0.003(0)	0.0017(4)	–0.0007(4)	0.0256(3)
B^P	0.77299(15)	0.87807(13)	0.60886(6)	0.0126(4)	0.0134(4)	0.0165(4)	0.0033(3)	0.0006(3)	–0.0001(3)	0.0141(2)
O1	0.8335(18)	0.2703(15)	0.9214(6)	0.018(5)	0.015(5)	0.006(4)	–0.003(4)	0.004(3)	0.001(4)	0.014(2)
O2	0.5604(18)	0.1189(15)	0.7654(7)	0.015(5)	0.013(5)	0.020(5)	0.003(4)	0.001(4)	–0.004(4)	0.016(2)
O3	0.0539(17)	0.1205(14)	0.7674(7)	0.007(4)	0.012(4)	0.020(5)	0.005(4)	0.001(3)	0.006(3)	0.013(2)
O4	0.8059(17)	0.4347(14)	0.7686(7)	0.011(4)	0.005(4)	0.022(5)	–0.001(4)	0.000(4)	0.000(4)	0.0130(19)
O5	0.5574(17)	0.7437(14)	0.7694(7)	0.012(4)	0.014(5)	0.016(4)	0.007(4)	0.002(4)	0.002(4)	0.014(2)
O6	0.0543(17)	0.7438(14)	0.7700(7)	0.009(4)	0.011(4)	0.019(5)	0.008(4)	0.002(3)	0.001(4)	0.0123(19)
O7	0.8364(17)	0.6861(15)	0.9226(7)	0.009(4)	0.016(5)	0.014(4)	0.001(4)	–0.001(4)	0.002(4)	0.013(2)
X^O_M	0.6535(19)	0.018(2)	0.0831(7)	0.013(5)	0.046(7)	0.019(5)	0.004(5)	–0.001(4)	0.006(5)	0.026(3)
X^O_A	0.289(2)	0.4766(19)	0.9268(8)	0.042(7)	0.026(6)	0.030(6)	0.003(5)	0.014(5)	0.004(6)	0.032(3)

O8	0.985(2)	0.1988(16)	0.5540(7)	0.019(5)	0.027(6)	0.019(5)	0.007(4)	0.001(4)	–0.001(4)	0.021(2)
O9	0.5357(18)	0.1999(15)	0.5532(7)	0.011(4)	0.019(5)	0.023(5)	0.004(4)	0.001(4)	0.001(4)	0.018(2)
O10	0.733(2)	0.2673(17)	0.4186(8)	0.020(5)	0.034(6)	0.027(6)	0.021(5)	–0.002(4)	–0.003(5)	0.025(3)
O11	0.765(2)	0.4949(16)	0.5724(13)	0.009(5)	0.004(5)	0.117(13)	–0.011(7)	–0.006(6)	–0.004(4)	0.046(4)
Subsidiary peaks*										
1	0.646(8)	0.125(7)	0.392(3)	0.02**						
2	0.719(7)	0.015(5)	0.322(2)	0.02**						

*Site occupancies for 1 and 2 are 0.02 and 0.03, respectively (scattering factor of Ba); **U_{iso}

Table 5. Selected interatomic distances (Å) and angles (°) for ferroinnelite.

Si1–O2	1.62(1)	Si2–O7	1.61(1)		T–O11	1.49(1)	
Si1–O1	1.62(1)	Si2–O6a	1.62(1)		T–O9	1.50(1)	
Si1–O3a	1.63(1)	Si2–O5	1.63(1)		T–O10	1.51(1)	
Si1–O4	1.66(1)	Si2–O4	1.64(1)		T–O8	1.51(1)	
<Si1–O>	1.63	<Si2–O>	1.63		<T–O>	1.50	
Si1–O4–Si2		137.1(7)					
M^H–X^O_M	1.70(1)	M^O1–(X^O_A)d	1.95(1)	×2	M^O2–(X^O_M)e	2.31(1)	×2
M^H–O5c	1.96(1)	M^O1–O1c	2.02(1)	×2	M^O2–O7c	2.48(1)	×2
M^H–O6c	1.97(1)	M^O1–O7c	2.03(1)	×2	M^O2–O1c	2.51(1)	×2
M^H–O3b	1.97(1)	<M^O1–φ>	2.00		<M^O2–O>	2.43	
M^H–O2b	1.97(1)						
<M^H–O>	1.91	A^P–O8e	2.68(1)		B^P–O11	2.69(1)	
		A^P–O9	2.68(1)		B^P–O9c	2.79(1)	
M^O3–O1f	2.22(1)	A^P–O10c	2.80(1)		B^P–O8h	2.80(1)	
M^O3–O7	2.22(1)	A^P–O5	2.83(1)		B^P–O8i	2.80(1)	
M^O3–(X^O_A)f	2.26(1)	A^P–O6	2.83(1)		B^P–O9h	2.81(1)	
M^O3–X^O_A	2.26(1)	A^P–O2	2.99(1)		B^P–O10i	2.90(1)	
M^O3–(X^O_M)g	2.29(1)	A^P–O3	2.99(1)		B^P–O10c	2.90(1)	
M^O3–(X^O_M)c	2.37(1)	A^P–O4	3.01(1)		B^P–O2h	2.97(1)	
<M^O3–φ>	2.27	A^P–O4e	3.01(1)		B^P–O5	2.99(1)	
		<A^P–φ>	2.87		B^P–O6a	2.99(1)	

	B^P–O3j	3.00(1)
	<B^P–φ>	2.88

φ = O, OH, F;
a: *x*+1, *y*, *z*; b: –*x*+1, –*y*, –*z*+1; c: –*x*+1, –*y*+1, –*z*+1; d: *x*, *y*, *z*–1; e: *x*–1, *y*, *z*;
f: –*x*+1, –*y*+1, –*z*+2; g: *x*, *y*+1, *z*+1; h: *x*, *y*+1, *z* ; i: –*x*+2, –*y*+1, –*z*+1; j: *x*+1, *y*+1, *z*.

Table 6. Refined site-scattering values and assigned site-populations for ferroinnelite.

Site*	Refined site-scattering (epfu)	Assigned site-population (*apfu*)	Calculated site-scattering (epfu)	<X–φ>$_{obs.}$** (Å)	Ideal composition*** (apfu)
		CATIONS			
$^{[5]}M^H$	44.0	$Ti_{1.98}Al_{0.02}$ $Ti_{1.97}Nb_{0.02}Al_{0.01}$	43.82	1.92	Ti_2
M^O1	22.6(3)	$Ti_{0.93}Nb_{0.05}Zr_{0.01}Mg_{0.01}$ $Ti_{1.00}$	23.03	2.00	Ti
M^O2	11.0	$Na_{1.00}$ $Na_{1.00}$	11.00	2.45	Na
M^O3	33.0(5)	$Na_{0.95}(Fe^{2+}_{0.64}Mg_{0.21}Mn^{2+}_{0.19}Ca_{0.01})_{\Sigma 1.05}$ $Na_{1.16}(Mn^{2+}_{0.38}Fe^{2+}_{0.17}Mg_{0.15}Ca_{0.10}\square_{0.04})$	34.56	2.27	$(NaFe^{2+})$*** $(NaMn^{2+})$
$^{[4]}T$	28.4	$S_{0.94}P_{0.89}\square_{0.17}$ $S_{1.02}P_{0.81}\square_{0.17}$	28.39	1.50	(SP)
$^{[9]}A^P$	109.4(5)	$Ba_{1.92}Sr_{0.07}Na_{0.01}$ $Ba_{1.97}Sr_{0.03}$	110.29	2.88	Ba_2
$^{[11]}B^P$	108.4(4)	$Ba_{1.92}Sr_{0.06}Na_{0.02}$ $Ba_{1.97}Sr_{0.03}$	110.02	2.88	Ba_2
$\Sigma A^P,B^P$	217.8	$Ba_{3.84}Sr_{0.13}Na_{0.03}$	220.76		Ba_4
$^{[4]}Si$(1,2)		Si_4			Si_4
		ANIONS			
O(1–7)		O_{14} →			$(Si_2O_7)_2$
X^O_M		O_2			O_2
$^{[3]}X^O_A$		$[O_{1.04}(OH_{0.85}F_{0.11})_{\Sigma 0.96}]_{\Sigma 2}$ $[O_{0.80}(OH_{0.99}F_{0.21})_{\Sigma 1.20}]_{\Sigma 2}$			[O(OH)]
O(8–10,$^{[2]}$11)		$[O_{7.32}(OH)_{0.51}(H_2O)_{0.17}] \rightarrow [(SO_4)_{0.94}(PO_4)_{0.89}(OH)_{0.51}(H_2O)_{0.17}]$ $[O_{7.32}(OH)_{0.51}(H_2O)_{0.17}] \rightarrow [(SO_4)_{1.02}(PO_4)_{0.81}(OH)_{0.51}(H_2O)_{0.17}]$			$[(SO_4)(PO_4)]$

* Coordination numbers are given for non-[6]-coordinated sites;
** φ = O, OH, F, H_2O;
*** Compositions and ideal compositions at all sites in ferroinnelite are respectively similar and equivalent to the ones in innelite-1*A* (shown in blue), except for the M^O3 site: $(NaFe^{2+})$ (ferroinnelite) and $(NaMn^{2+})$ in innelite-1*A* (Sokolova *et al*., 2011; Sokolova and Cámara, 2017).

Table 7. Bond-valence* (vu) values for ferroinnelite.

Atom	Si1	Si2	M^H	M^O1	M^O2	M^O3	T	A^P	B^P	Σ
O1	1.01			$0.57^{x2}\downarrow$	$0.15^{x2}\downarrow$	0.27				2.00
O2	1.01		0.64					0.15	0.16	1.96
O3	0.98		0.64					0.15	0.15	1.92
O4	0.91	0.95						0.15 0.15		2.16
O5		0.98	0.65					0.23	0.15	2.01
O6		1.01	0.60					0.23	0.15	2.02
O7		1.03		$0.56^{x2}\downarrow$	$0.16^{x2}\downarrow$	0.27				2.02
X^O_M			1.37		$0.22^{x2}\downarrow$	0.24 0.20				2.03
$^{[3]}X^O_A$**				$0.68^{x2}\downarrow$		0.26 0.26				1.20
O8							1.23	0.34	0.25 0.25	2.07
O9							1.27	0.34	0.25 0.24	2.10
O10							1.23	0.24	0.19 0.19	1.85
$^{[2]}$O11**							1.31		0.33	1.64
Sum	3.91	3.97	3.94	3.62	1.06	1.50	5.04	1.98	2.31	
Aggregate charge	4.00	4.00	3.99	4.03	1.0	1.53	5.05	2.00	2.00	

* Bond-valence parameters are from Brown (1981);
** Coordination numbers are given for non-[4]-coordinated anions.

Table 8. Comparison of ferroinnelite and innelite-1*A*.

Mineral	ferroinnelite[1]	innelite-1*A*[2]	
Ideal structural formula	Ba_4Ti_2 Na(NaFe^{2+})Ti $(Si_2O_7)_2[(SO_4)(PO_4)]O_2[O(OH)]$	Ba_4Ti_2 Na(NaMn^{2+})Ti $(Si_2O_7)_2[(SO_4)(PO_4)]O_2[O(OH)]$	
a (Å)	5.3994(8)	5.4234(9)	
b	7.09239(13)	7.131(1)	
c	14.7345(4)	14.785(3)	
α (°)	98.4086(19)	98.442(4)	
β	94.3275(18)	94.579(3)	
γ	90.0133(13)	90.009(4)	
V (Å^3)	556.56(8)	563.7(3)	
Space group	$P\bar{1}$	$P\bar{1}$	
Z	1	1	
$D_{calc.}$ (g cm^{-3})	4.088	4.024	
$D_{meas.}$ (g cm^{-3})		3.96	
Strongest reflections in the X-ray powder diffraction data, *d*/Å (I)	2.694(100)	2.9049(100)	14.7(100)
	3.353(56)	14.327(95)	2.709(100)
	2.124(46)	2.6857(79)	2.140(90)
	14.56(38)	4.831(51)	3.37(80)
	3.93(22)	3.247(44)	2.810(70)
	2.776(19)	2.1277(42)	4.20(40)
optical class, sign	biaxial (+)	biaxial (+)	
α	>1.800	1.726	
β	>1.800	1.737	
γ	>1.800	1.766	
2V (meas.) (°)	87(2)	82	
Locality	Kovdor massif, Russia	Inagli massif, Russia	

[1] this work;
[2] ideal structural formula, $D_{calc.}$, unit-cell parameters and space group are from Sokolova *et al.* (2011); $D_{meas.}$ and optical data are from Kravchenko *et al.* (1961), power-diffraction data are from Raade and Berg (2000) (powder diffractometer Siemens D5005, left) and Pekov *et al*. (2006) (RKU-86 mm camera, right).